

Reducing the carbon footprint of house heating through model predictive control – A simulation study in Danish conditions

P.J.C. Vogler-Finck^{a,b,*}, R. Wisniewski^b, P. Popovski^b

^a Neogrid Technologies ApS, Niels Jernes Vej 10, 9220 Aalborg Ø, Denmark

^b Department of Electronic Systems at Aalborg University, Fredrik Bajers Vej 7, 9220 Aalborg Ø, Denmark

ARTICLE INFO

Keywords:

Carbon footprint
Heating
Single-family house
Model predictive control

ABSTRACT

Around the world, electricity systems are transitioning towards renewable energy to meet humanity's climate change mitigation targets. However, in a pre-transition system, the carbon intensity of power exhibits strong variations over time, which calls for load shifting to times when its impact is lower. In this work, the case of heating in single-family houses is studied, using Model Predictive Control (MPC) to optimise multi-zone operation. Low inertia heating is used, and simulations are made upon three different insulation level using historical grid and climate data from Denmark. The results show that energy and CO₂ optimisation are relevant objectives for predictive control for lowering the carbon footprint of heating, while SPOT price optimisation is comparatively undesirable. However, benefits of energy optimisation were questioned, as a well-tuned PID control might have had similar performance. Nevertheless, gains from CO₂ optimisation in recent houses highlight the importance of considering the average carbon intensity of energy used, in addition to the amount of energy itself, when aiming to reduce the carbon footprint.

1. Introduction

1.1. Carbon emissions from the power sector

In Europe, a pathway for the energy transition to a low carbon¹ energy system has been traced by the European Union (European Commission; European Commission). As a member state, Denmark is following this roadmap, and therefore aiming at improving the energy efficiency of its energy sector, and reducing the related greenhouse gas emissions.

The Danish power system is well interconnected to Sweden, Norway and Germany. This allowed it to be among the frontrunners in integration of renewable energy in the power system, especially for wind power. In 2016, 63% of its electricity generation was from renewable sources (43% wind, 18% biofuels and waste, and 2% solar), while 29% was from coal (IEA). Therefore, dynamic variations of the carbon intensity of power are often observed due to fluctuations of the respective shares of coal and renewables. This is illustrated in Fig. 1 for the period 2013–2016, showing up to a factor 3 between lowest and highest carbon intensity (as well as an overall slow downward trend as fossil fuels are progressively phased out).

In the transition phase towards fully renewable electricity systems,

it is expected that such dynamic variations of carbon intensity will become more widespread around the world. Therefore, it is important to study the impact of dynamic variations in carbon intensity, and applications of load shifting to times with lower carbon intensity.

1.2. Residential buildings as actors in the energy transition

Introduction of energy flexibility in dwellings should allow introducing more variable renewable generation in electricity systems (Lund et al., 2015), and provides capacity for load shifting. In particular, heating, ventilation and air-conditioning (HVAC) loads constitute a major part of the demand (more than a third for countries of the Major Economies Forum on Energy and Climate Change (IEA, IEA, IPEEC, 2015)).

In Denmark, a major part of this electricity is consumed in residential buildings (32.1% in 2015 (IEA, 2017)). However, only a small fraction of this residential load is for heating purposes (around 4% in 2015 (IEA, 2017), but expected to grow as oil boilers are phased out). In the specific case of Denmark, the largest part of residential heating is coming from district heating (43% in 2015 (IEA, 2017)). However, other countries are (or may become, as a result of their energy transition) significantly more reliant upon electrical heating in the residential

* Corresponding author at: Neogrid Technologies ApS, Niels Jernes Vej 10, 9220 Aalborg Ø, Denmark.

E-mail address: pvf@neogrid.dk (P.J.C. Vogler-Finck).

¹ In this work, 'carbon' is used as a synonym for 'greenhouse gas emissions'.

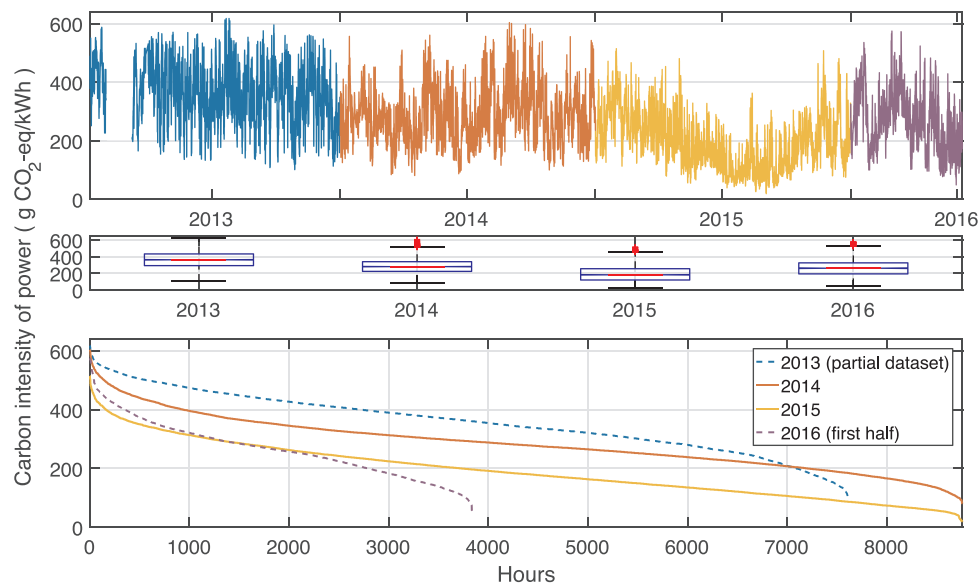


Fig. 1. Carbon intensity of the power in Denmark for the period 2013–2016, at transmission level (data from *Styr din Varmepumpe* (SdVP, in press), provided by Energinet: the Danish transmission system operator (TSO).)

sector.

It is important to control these HVAC loads in the most efficient and meaningful way, while making use of the flexibility in their energy usage to provide benefits to the overall energy system. This can be addressed by using model predictive control (MPC).

In this paper, we investigate the value of MPC applied to single-family house heating with a low inertia heating system. Different strategies for MPC are considered (aiming at minimising either energy use, indirect CO₂ emissions (footprint), cost, or discomfort) and compared to a classic thermostatic heating. Moreover, the analysis is carried out on different house ages to evaluate the impact of their insulation level on the conclusions.

1.3. Related work on model predictive control of HVAC in households

Predictive control of HVAC systems in buildings has been extensively researched in the recent decades, with some early works prior to the nineties (Nygård Fergusson, 1990). An overview of the field is found in several reviews (Dounis and Caraiscos, 2009; Shaikh et al., 2014; Afram and Janabi-Sharifi, 2014) while a practical introduction to MPC may be found in Maciejowski's reference book (Maciejowski, 2002).

However, practical hurdles are still preventing widespread adoption of MPC. The main bottleneck, as highlighted by Prívará et al. (2012), is the identification of a reduced order model for the purpose of control. Identification of such a model has been extensively studied using different modeling approaches. So-called 'grey-box' models combining physical insight and local measurements in operation (Jiménez et al., 2008; Bacher and Madsen, 2011; Delf Andersén et al., 2014; Reynders et al., 2014; De Coninck, 2015; Fonti et al., 2017; Ferracuti et al., 2017) are typically preferred for its robustness and the limited amount of data required, with a toolbox for model development and validation introduced by De Coninck et al. (2015). However, other so-called black-box' approaches such as artificial neural networks (Morel et al., 2001; Vinther et al., 2017) and subspace methods (Prívará, Široký et al., 2011) are also found in the literature. More insight in the field of identification of control-oriented models of buildings for HVAC control is found in the reviews from references (Prívará et al., 2012; Li and Wen, 2014; Atam and Helsen, 2016), and a theoretical introduction to model identification is provided in Ljung's reference book (Ljung, 1999).

MPC of heating is mostly operated using mathematical optimisation in implicit forms, requiring the use of optimisation solvers online (although some attempts to adopt an explicit approach to the optimisation have been made – e.g. in references (Drgona et al., 2013; Fabietti, 2014)). Therefore, the complexity of the optimisation must remain low, so that they can be solved in real-time on hardware with limited computational power. In particular, detailed models can hardly be used in optimisation, as the complexity of the optimisation would be dramatically increased.²

Recent developments in the field arose from the interaction with the 'smart grid' research field, beyond the traditional building-centred indoor comfort focus of prior works in building climate management. It resulted in increased attention being given to the potential for provision of services to the power system by using MPC for HVAC load control (De Coninck, 2015; Oldewurtel, 2011; Maasoumy Haghighi, 2013; Bianchini et al., 2016). For the particular case of heat pumps, a review is found by Fischer and Madani (2017).

As highlighted in the review from Clauß et al. (2017), a variety of objective functions can be used in MPC, depending on the aim of the control designer. Typical examples are minimisation of energy use and maximisation of comfort (measured by the deviation from a set-point, either in absolute or quadratic deviation), but also objectives considering the dynamics of the broader energy system such as energy price (Masy et al., 2015) or CO₂ emissions (Knudsen and Petersen, 2016). A prior study in the case of single-family house heating with an idealised MPC highlighted significant differences in behaviour and performance depending on the chosen objective (Vogler-Finck et al., 2017).

Some works are also starting to look into combination of the different objectives. For example, Knudsen and Petersen (2016) investigated heating of a dormitory room using MPC with an objective function considering a weighted sum of day-ahead real-time price and carbon intensity. Variation of the weights allowed quantification of trade-offs between CO₂ and price.

In a review of the literature on heating control adopting a building-centred perspective, Nägele et al. (2017) found that both comfort and

² This is because the number of equality constraints in the optimisation programs is proportional to the number of states in the model multiplied by the optimisation horizon length. It is also worth mentioning that state estimation is also problematic for detailed models with a limited set of measurements.

energy use are relevant performance metrics. Energy use was addressed using net heating requirements, including sun, appliances and excluding pipe losses. Comfort was addressed by counting the number of hours where the indoor comfort was unsatisfactory (defined as $PPD > 10\%$, using the PPD definition from ISO 7730 (EN ISO, 2005)). However, it is also important to adopt a wider point of view and integrate energy system considerations in the performance assessment (Clauß et al., 2017). In particular, the total CO₂ emissions originating from the energy production is essential to the environmental impact assessment. Moreover, it was noted by Clauß et al. (2017) that MPC studies in the literature mainly focus on the precise metrics they are aiming at optimising, often introducing risks of undesirable blind trade-offs (in particular on the carbon footprint studied here).

When it comes to the study of the impact of building age on the benefits and performance of implementation of MPC, Masy et al. (2015) carried out simulations assessing the influence of different insulation levels (in Belgian climate). Pedersen et al. (2017) also investigated the impact of demand response potential from apartment buildings with different retrofit levels in a Danish context using economic MPC, including a study of tradeoffs between energy costs and emissions. However, such studies are few and it seems that there is considerable room for research on the topic. Thus, the impact of the house insulation level on the conclusions was also considered in this study.

1.4. Contribution of the work

The contributions of this article are fourfold, in the context of low inertia heating of a single-family house, using a simple deterministic simulation model.

- First, a two level controller based upon model predictive controller at building level, and dispatch of the resulting power within the different zones is presented. This allows ensuring comfort in a multi-zone building with a single zone MPC optimisation, which has the advantage of requiring significantly lower modelling effort.
- Second, a quantification of the benefits of implementation of MPC (compared to thermostatic control) for low inertia heating is presented, including reductions in CO₂ emissions from electricity used. It is shown that the value of MPC varies throughout the year and with house age.
- Third, a critical comparison of the possible objective functions is made, highlighting trade-offs between energy use and CO₂ footprint and questioning the relevance of price and comfort optimisation for MPC.
- Lastly, a novel metric for flexible load operation is proposed: the *average carbon intensity of the power consumed*.

2. Methodology

In this part, the methodology of the work is presented.

2.1. Single-family house models

In this subsection, the simulation model of the single-family house is presented. Focus is made on a single-family house, as these are typical residential buildings outside the areas covered by district heating in Denmark.

2.1.1. Building simulation model

This study uses 3 single-family house models developed in the third-party project OPSYS (OPSYS). These houses have identical geometry (4 rooms and a total area of 150 m², see Fig. 2), but different levels of insulation and ventilation (corresponding to a building from 1970, 2010, and 2015).

The models are based upon linear differential equations, with the same structure in the 3 cases, but different values of their numerical

parameters. More details about the model structure, parameters, and inputs are found in the report of the Opsys project (Jensen, 2017).

These models account for effects from ambient temperature and vertical components of the solar radiation for each direction (north, south, east and west). Internal doors movement and heat gains from appliances and people (see Fig. 3) are integrated in the model through weekly schedules, using values from the report (Jensen, 2017). Occupancy profile was derived from internal heat gains, as the building was considered occupied whenever one of the following conditions on the internal heat gains values was true: above 150 W in room 1, above 50 W in room 2, above 40 W in room 3, or above 25 W in room 4. Influence from the wind, humidity and atmospheric pressure is not modelled.

As the model is meant for heating studies, analysis was restricted to the heating period for each of the 3 buildings. It is important to note that these periods differed among building ages, due to differences in their insulation, as discussed below.

The heating source and its control were added, as they were not included in the original model from OPSYS. In each room, the heating is modelled as an electrical radiator heating (dimensioned according to the criteria described later in this article), with a power to heat conversion efficiency of 1, and an assumption that all its heat output is released into the air of the room.

The simulation model is implemented in MATLAB. Differential equations in the model are solved using the forward Euler method, with a short time-step of $T_s = 1 \text{ min}$ to minimise numerical errors.³ Control updates for the heating source are then updated in a slower manner (every 5 min for the thermostats and dispatcher, and 30 min for the MPC to reflect computational constraints), and zero order hold is applied to the set-points in order to allow for simulation with steps of 1 min.

2.1.2. Input and disturbance data

Weather and power system data for the period December 2014 to January 2016 was obtained from the project *Styr din varmepumpe* (SdVP, in press).

The weather data originate from the *Danish Meteorological Institute*, and includes hourly values of ambient temperature, and solar radiation (both direct horizontal and diffuse components) which were used as model inputs and are presented in Fig. 4 below. Vertical components of the direct solar radiation were derived using the method presented in the textbook by [Twidell and Weir, 2006, chap. 4 (pp. 89–95)]. Diffuse radiation was integrated in the model by adding half the value to each of these vertical components (reflection from ground is neglected here). Ground temperature was not available in the dataset. Therefore, a constant value of 10 °C was used, in accordance with the model description (Jensen, 2017). Although wind speed and humidity data were available, these were not considered in the model.

The power system data plotted in Fig. 5 originate from the Danish transmission system operator *Energinet*. These include hourly values of the SPOT price of the power, carbon intensity of the power (i.e. the equivalent amount of CO₂ emitted per unit of energy consumed). Occasional missing data were replaced by the average of the signal, in order to be able to operate the simulations.

The carbon intensity is computed using the methodology provided in Energinet's report (Energinet, 2017), and applies at transmission level. For conversion to the distribution level where the house is connected, a 5% loss in the distribution network was then assumed in all footprint calculations below (consistently with the average value proposed in the methodology (Energinet, 2017)).

2.1.3. Dimensioning of the heating system and heating season

For all 3 houses, the heating capacity was dimensioned using the

³ Higher order methods such as Runge-Kutta methods or exact discretisation would provide more accurate results.

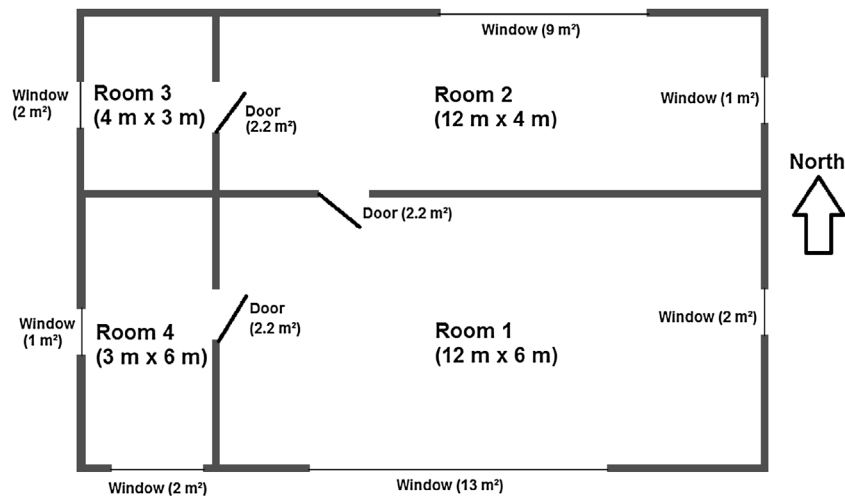


Fig. 2. Layout of the 3 buildings (adapted from Jensen (2017) and Vinther et al. (2017)).

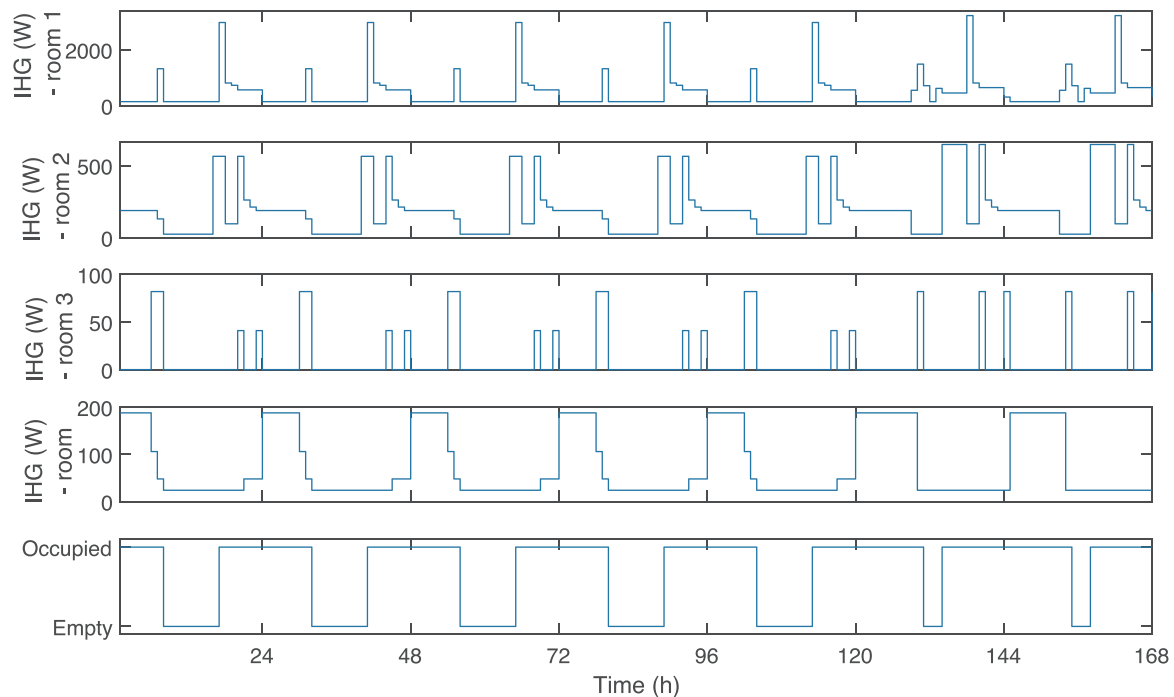


Fig. 3. Weekly schedule of internal heat gains (data from Jensen (2017)) and occupancy.

Danish standard DS 469 (DS 469, 2013). This standard requires that the heating must be able to maintain an indoor temperature of 20 °C with an ambient temperature of −12 °C (a conservative approach was adopted here, as we removed internal heat gains and solar gains when computing this capacity).

The resulting total heating capacities varied within 2.4–7.3 kW for the 3 houses, due to their differing insulation, as shown in Table 1. This total capacity was then divided among the rooms according to their fraction of the total floor area. While this splitting differs from the one obtained by computing the room heating capacity required to meet the design requirements, their differences are in the range of average internal heat gains (rooms 3 and 4 with lower internal heat gains tend to be over-dimensioned, and room 1 with large solar and internal heat gains tends to be under-dimensioned), so that it is a reasonable approximation.

Heating periods were computed for each of the 3 buildings separately, as their insulation levels resulted in different heat needs. This was made using thermostatic control on data from the whole year, and

then manually identifying when the heat load was insignificant. Resulting periods are given in Table 1.

2.1.4. Comfort considerations

Comfort bounds were defined on the indoor air temperature, accordingly with the standard EN 15251 (ENDS, 2007, Appendix A3). Here, all 4 rooms are assumed to be hosting sedentary activities. This corresponds to a comfort range of 18–25 °C for the 1970 house (considered as an *existing building*), and 20–25 °C for the 2010/2015 houses (considered as *renovated/new buildings*).

In order to allow for realistic simulations and comfort in the inter-season, window opening is implemented in each of the rooms. These windows are controlled using the simple condition that a window is opened whenever the building is occupied, and the air temperature is above 27 °C for the 1970 house and 26 °C for the 2010/2015 houses (accordingly with the temperature upper limit for cooling in sedentary activity rooms in residential buildings consistently with the above use of EN 15251 (ENDS, 2007)). It is however important to remember that,

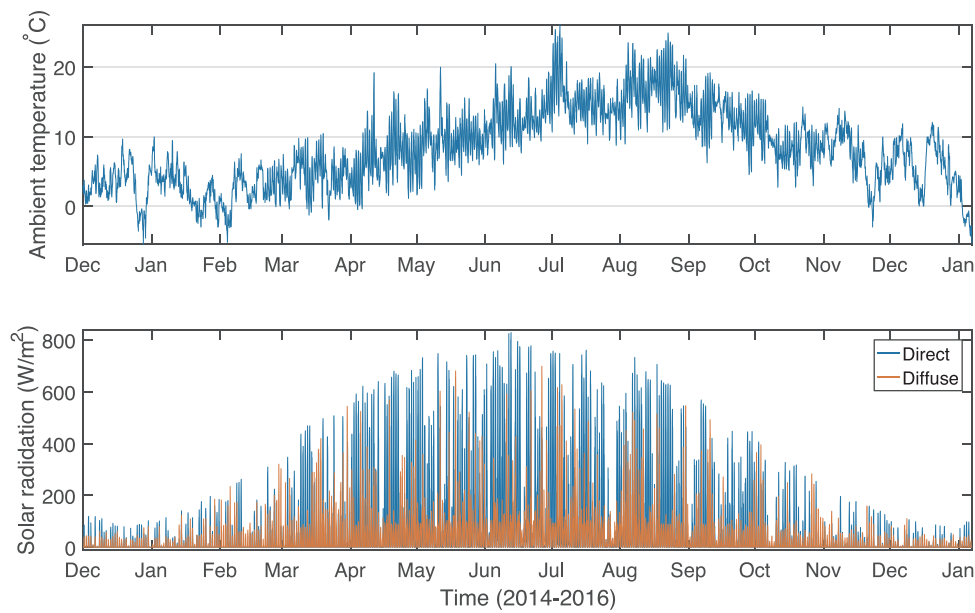


Fig. 4. Weather data (data from *Styr din Varmepumpe SdVP*, in press).

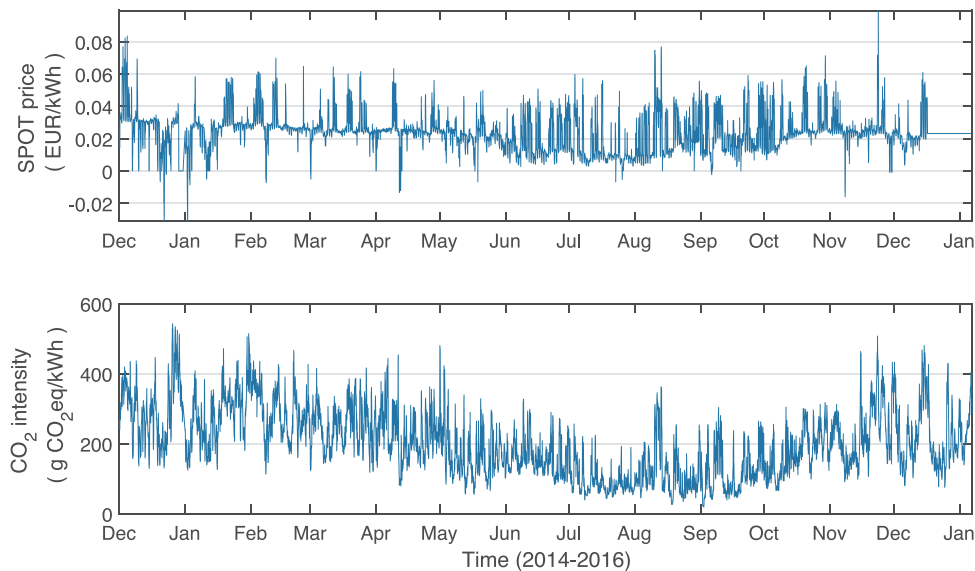


Fig. 5. Power system data (data from *Styr din Varmepumpe SdVP*, in press).

Table 1
Heating seasons and dimensioning by house age.

Age	Heating period	Capacity
1970	January–December (365 days)	7.3 kW
BR10	January–April 18th and October–December (200 days)	3.1 kW
BR15	January–March and October–December (182 days)	2.4 kW

as highlighted by Andersen et al. (2013), window opening patterns depend on a variety of parameters, such as indoor CO₂ concentration and relative humidity (even potentially wind speed, although its significance seems doubtful according to some studies (Andersen et al., 2013, 2009)).

Whenever the window is opened, an air flow to ambient air is added for the simulation step, following the empirical relationship used in reference Vinther et al. (2017):

$$V_{\text{window}} = \alpha A_{\text{window}} V_f \quad (1)$$

where α is the opening fraction (set to 0.5), A_{window} is the window area, V_f is the F-area flow (set to 0.1 m³/m²/s, consistently with the Opsys model definition (Vinther et al., 2017)).

It is worth noting that such comfort bounds differ between standards, and adjustment would probably be left to users in practice. For example, the Danish standard DS 469 (DS 469, 2013) recommends a much tighter bound of 20–22 °C in living spaces of residential buildings in heating conditions (21–23 °C in bathrooms). Here, it is also important to remember that user preferences often differ from standards. For example, a survey in a Danish context that most respondents estimated their living room temperature to be within 20–22 °C and bedrooms to be below 20 °C (Knudsen, Andersen, et al., 2016). In another study made in a British context, a notable tendency for under-heating in rooms (compared to standard requirements) was also observed (Dyson, 2016).

2.2. Baseline controller

In this study, the baseline controller of the heater in each room is a

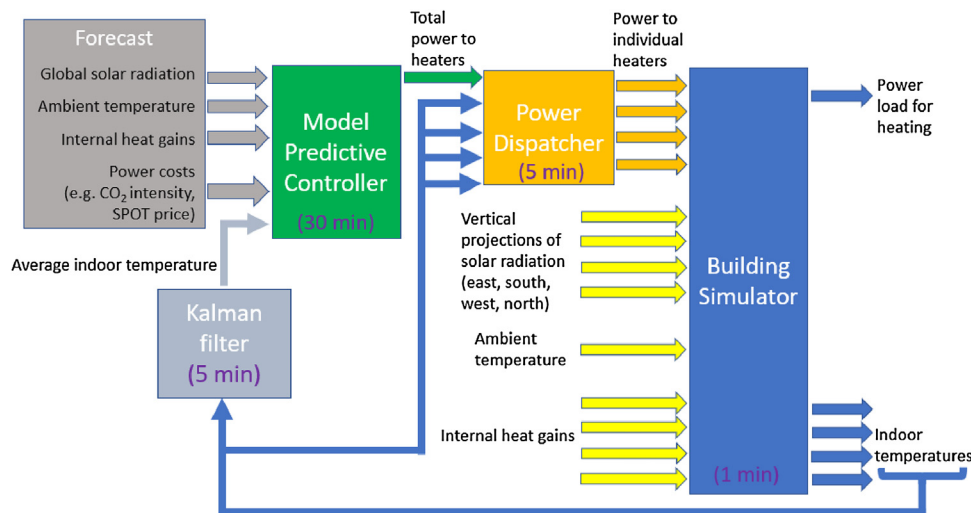


Fig. 6. Structure of the 2 stage advanced controller combining MPC and dispatching (durations in every block indicate update/sample time).

simple thermostatic controller. It operates using the indoor air temperature of the room as a feedback. It is forced to stop if a window is open in the room or if the period is out of the heating season (as defined in Table 1).

Two sets of thermostatic settings are considered: a ‘high consumption’ type with *start-stop* room temperatures of 22–23 °C (designated as ‘TH-HOT’ below), and a ‘low consumption’ type (comparable to the lower bound of the MPC) operating in the range 21–22 °C (designated as ‘TH-REF’ below, and used as a baseline).

2.3. Model predictive controllers

A MPC controller was implemented, using a linear programming approach in order to represent future practicable potential.

Different strategies were compared for the control formulation:

- **Energy-optimising** (‘MPC-EN’ below): the objective function is the total energy used over the optimisation horizon;
- **CO₂-optimising** (‘MPC-CO₂’): the objective function is the total indirect CO₂ emissions over the optimisation horizon;
- **Price-optimising** (‘MPC-SPOT’): the objective function is the total SPOT price over the optimisation horizon (the actual power price is used, rather than day-ahead predictions of it);
- **Comfort-optimising** (‘MPC-COMF’): the objective function is the total integrated deviation of the average indoor air temperature from a reference of 22 °C.

It is important to note that actual values of price and carbon intensity are used in this study, while in practice predictions would be used in the controller (prediction of future prices and carbon intensity at each time-step was not available in our historical data). Dependency of the control performance to the quality of the prediction is therefore out of the scope of this study (although it is an important factor which should be assessed in future studies), which provides an estimate of the upper bound on performances.

A deliberate choice to focus on linear programming optimisation for the whole control chain is made, as such optimisation problems are well-known, and a variety of solvers is available to solve them (including open source tools (Gearhart et al., 2013)).

The control operated with these advanced controllers consists in a combination of a single thermal zone optimisation (using traditional MPC), and a power dispatcher to the individual rooms. This is summarised in Fig. 6 below, whose components are introduced in the paragraphs below.

2.3.1. Reduced order model

The building thermal dynamics were modelled by a simple continuous time linear state space model. This model approximates the building to a single thermal zone, and takes the following form:

$$dX(t) = [A X(t) + B_U U(t) + B_V V(t)] dt + K d\omega(t) \quad (2)$$

$$Y(t) = C X(t) + D_U U(t) + D_V V(t) + e(t) \quad (3)$$

where X is the state vector (composed of the average room temperature in the building, and some potential hidden states), U the controlled inputs vector (containing the total power to the heaters), V the disturbance vector (ambient temperature, internal heat gains, and vertical component of the global solar radiation), Y the observation vector (containing the average of indoor temperatures from simulated sensors reacting to changes in the air temperature with a 2 min time constant), e is a noise vector (assumed to be white noise), ω a Wiener process,⁴ and (A , B_U , B_V , K , C , D_U , D_V) are the linear state-space model matrices. The identification of the latter matrices is discussed in the next sub-section.

The degree of opening of the doors has a significant impact on heat transfer coefficients between rooms (e.g. neglecting heat capacity of the wall, the heat transfer coefficient of room 1 to 2 was 43 W/K with closed door, and 164 W/K with 50% open door). An optimal controller optimising the 4 different radiator power inputs would therefore need to have knowledge of the state of these doors (including their future values) to be capable of reliable predictions, which is not realistic. Moreover, such a multi-zone model comprises a large number of states and parameters, which makes it complicated to identify in practice.

For these reasons and to reflect achievable field deployment, it was chosen to identify a simple *single zone* dynamical model, and assume that the opening of the doors was unknown to the controller. Then, a dispatcher layer is added in order to split the result of the optimisation among the 4 zones. These reduced control-oriented models and dispatching of heating are presented in the next subsections.

2.3.2. Identification of the control model

The implementation of the predictive controller requires an identification of the model described in Eq. (2). Here, it was chosen to use a grey-box modelling approach, rather than using the detailed knowledge of the building implemented in the simulator. This is because the objective is to replicate similar conditions to the model fidelity which is achievable in practice.

⁴ Here, a stochastic description is only used in modelling and state estimation (using the Kalman filter). The MPC will use a certainty equivalent deterministic model.

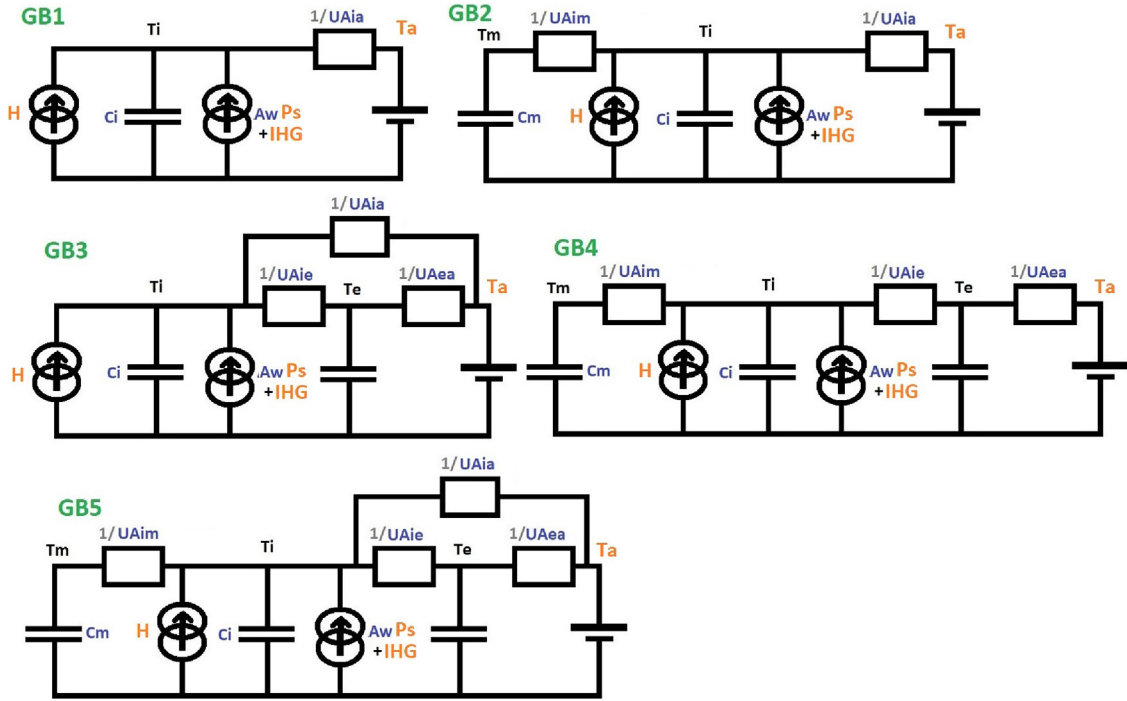


Fig. 7. Grey-box models investigated for the controller in RC network form (parameters are shown in blue, output is the average indoor air temperature T_i , inputs are the total amount of power to heater H , global solar radiation P_s , internal heat gains IHG , and ambient temperature T_a). (For interpretation of the references to color in this figure legend, the reader is referred to the web version of this article.)

Several approaches were compared for each of the 3 buildings, using the MATLAB System Identification toolbox (Ljung, 2016). This model identification was made upon data that were generated by applying a *pseudo-random binary sequence* to the heaters of the building in the simulator, similarly to Bacher and Madsen (2011). Simulation was made over 28 days using input data from December 2014, and disabling internal heat gains and window opening (to replicate an empty building set-up), with a 1 minute step similarly to further simulations. Subsequently, the dataset was resampled to 15 min samples (using averaging) prior to usage in the toolbox in order to reflect good experimental practice (Madsen et al., 2016).

Five different continuous time grey-box models of increasing complexity were tested (GB1, GB2, GB3, GB4, GB5 – where the number increases with complexity, see Fig. 7). As often made in grey-box modelling of buildings, continuous time is used here in order to ensure physical interpretation of the parameters, allow easy resampling of the model to different discrete sample times.

For the 3 houses, the toolbox was able to identify parameters for all 5 models (GB1, ..., GB5), using the ‘greyest’ method in continuous time. However, only the first order model (GB1) had standard deviations that were low for all parameters. For other models, some of the parameters of the envelope were observed to come with large uncertainty. Despite these uncertainties, it was decided to assess their performance for control, compared to a well-identified first order model. Results show that these could indeed provide performance improvement in some cases.

The identified continuous time state space model (A , B_U , B_V from Eq. (2)) was then discretised to allow its use in the Kalman filter (5 min time step, to allow for a more precise and robust state-estimation to be used by the MPC) and the discrete time model predictive controller (30 min time step, resulting in the matrices $A^{(d)}$, $B_U^{(d)}$, $B_V^{(d)}$ below).

The fits of the models used later in the MPC were computed, using their discretised version with a sample time of 30 min and the R -squared as a fit metric on the dataset (the same dataset was used for training and validation, as the models are later compared in MPC experiments providing some sort of validation). For the 1970 house, the

GB5 model was used in MPC and had a fit of 93.7% for prediction 30 min ahead, and 75.2% for 24 h ahead. For the BR10 house (model GB4), this fit was 95.5% for 30 min ahead, and 92.3% for 24 h ahead. Lastly, for the BR15 house (model GB4), fits were 95.3% for 30 min ahead, and 55.1% for 24 h ahead prediction.

2.3.3. Single zone optimisation

At each time-step k when the model predictive controller is run, a *linear programming* problem is solved (using the linear programming solver from the solver Gurobi (Gurobi Optimization Inc., 2017)) over a N steps ahead horizon:

$$\min_{U[k] \dots U[k+N-1]} \sum_{j=0}^{N-1} (C_U[k+j]U[k+j] + C_X[k+j+1]\|X[k+j+1] - X_{\text{ref}}[k+j+1]\|_1 + \rho[k]\|\xi[j]\|_1) \quad (4)$$

$$\text{s. t. } X[k] = \hat{X}_k \\ \forall j \in \{0, \dots, N-1\}, \quad (5)$$

$$X[k+j+1] = A^{(d)}X[k+j] + B_U^{(d)}U[k+j] + B_V^{(d)}V[k+j] \quad (6)$$

$$0 \leq U[k+j] \leq P_{\text{rated}} \quad (7)$$

$$X_{\text{min}}[k+j+1] - \xi[j] \leq X[k+j+1] \leq X_{\text{max}}[k+j+1] + \xi[j] \quad (8)$$

$$0 \leq \xi[j] \quad (9)$$

Eq. (4) sets the objective of the optimisation, with C_U a scalar input cost, C_X a scalar discomfort cost penalising the deviation from a reference X_{ref} , ξ the deviations outside the comfort range and ρ a ‘large’ cost for these deviations (these were used to ensure feasibility of the optimisation at all times).

In Eq. (5), the initial state of the system is fixed to an estimated value \hat{X}_k . This estimated value is computed from observations of the room temperatures using the Kalman filter (with observation noise adjusted compared to its identified value). This filtering is required to compensate for the unobserved states modelling the thermal mass of the building structure in models GB2, GB3, GB4, GB5 (as well as coping

with missing measurements in real-world applications).

In Eq. (6), the expected future dynamics of the system are modelled using an equality constraint based upon the matrices corresponding to the discretised version of the model ($A^{(d)}$, $B_U^{(d)}$, $B_V^{(d)}$ – the noise description is dropped in the deterministic approach used here⁵).

Eq. (7) constrains the total power input to remain below the rated power of the heating P_{rated} , and above a minimum (cooling is not allowed).

Eq. (8) constrains the state to remain within lower X_{min} (21 °C) and upper X_{max} (24.2 °C) bounds. These constraints are softened by allowing deviations, which must remain positive (ensured by Eq. (9)) and discouraged (by the cost ξ in Eq. (4)).

Then, the first step of this ‘optimal’ sequence is applied and the optimisation is run again at the next step (hence the term ‘receding horizon’ sometimes used as an alternative to ‘model predictive control’). It is worth noting that the value of the inputs can vary within an interval, and is not limited to a discrete number of values. This allows to use linear programming (rather than its computationally-heavy mixed-integer extension) and can be justified by the fact that the heating can be only activated for a fraction of the considered period. In this work, a control step of $T_c = 30$ min is used.

Different possibilities for the input cost C_U and the state cost C_X were assessed in the study, corresponding to the above-mentioned strategies:

- Energy optimisation (MPC-EN): constant cost for $C_U[k] = 1$, and $C_X[k] = 0$ for all k .
- CO₂ optimisation (MPC-CO₂): the value of the carbon intensity of the power is used for C_U , and $C_X[k] = 0$ for all k .
- SPOT price optimisation (MPC-SPOT): the SPOT price of the power is used for C_U , and $C_X[k] = 0$ for all k .
- Comfort optimisation (MPC-COMF): $C_U[k] = 0$, and a constant cost is used for $C_X[k] = 1$ for all k .

At each step, the value of the ‘softening weight’ ρ was chosen according to the following equation:

$$\rho[k] = \frac{10}{N} \max \left(P_{rated} \left\| \begin{pmatrix} C_U[k] \\ \vdots \\ C_U[k+N-1] \end{pmatrix} \right\|_1, \left\| \begin{pmatrix} C_X[k+1] \\ \vdots \\ C_X[k+N] \end{pmatrix} \right\|_1 \right) \quad (10)$$

In simple terms, this means that, for a given step, the cost of deviating 1 °C from the constraints will be at least 10 times the average cost of consuming full power for one step, or deviating 1 °C from the temperature set-point. Here, ‘average’ is to be understood as the ‘average of the absolute value within the optimisation horizon of the MPC at time k ’.

2.4. Dispatching of the heat between zones

The result of the optimisation yields a total amount of power for the building heating (P_{MPC}), which is assumed to be converted to heat with an efficiency of 1. Then this total amount needs to be dispatched between the individual rooms, which is made using a heuristic approach.

As stated previously, the motivation for this combination of MPC and dispatch at room level is to overcome the dynamical modelling issue originating from the unknown door openings (strongly affecting the thermal coupling between zones), which is a barrier to a simple implementation of MPC directly at room level.

2.4.1. Ensuring minimal comfort level in each room

The MPC operates using the average temperature of the building.

⁵ This is consistent with the use of a Wiener process in Eq. (2), which has average 0

However, it happened that some of the rooms were too cold while the average temperature would be high enough for the MPC to keep the heating low or stopped.

Here, it is important to understand that this is not due to the poor predictions of the single zone model itself, but to the very limits of a single zone model approach. In such a multi-zone building with high internal gains in some rooms and limited coupling between rooms, indoor temperature can simply exhibit differences of several °C.

An upgrade of the dispatchers was therefore needed to guarantee a minimal heat input (P_{min}), by increasing the MPC output ($P_{MPC} = U[k]$ in Eq. (4)) where needed. In the following, delivery of such extra heat is named ‘boosting’. This was implemented using Algorithm 1, where full power is affected for the coming timestep to each heater in a room j where temperature falls below the minimum ($T_{min,j}$).

Algorithm 1. Dispatch upgrade to ensure minimal comfort in all 4 rooms.

Result: Minimal power to the heating ($P_{Dispatch}$)

```

 $P_{min} \leftarrow 0$ ;
for  $j$  from 1 to 4 do
    if  $T_j < T_{min,j}$  then
         $P_{min} \leftarrow P_{min} + P_{rated,j}$ ;
    end
end
 $P_{Dispatch} \leftarrow \max(P_{min}, P_{MPC})$ ;
return  $P_{Dispatch}$ ;

```

where in the case of these simulations, the same value of $T_{min,j}$ was used for all rooms (18.2 °C for the 1970 house, and 20.2 °C for the 2010 and 2015 houses, where the 0.2 °C is a margin to compensate thermal dynamics).

This ‘boosting’ potentially provides suboptimal increase of the energy use. However, it was observed that the share of the energy use originating from this suboptimal boosting is small (see Fig. 11).

2.4.2. Optimisation program

This balancing is operated using a heuristic approach relying upon linear programming optimisation and the solver from Gurobi (Gurobi Optimization Inc., 2017). Each time step, the controller splits the total heat between the individual rooms in a way that minimises the deviation between the room temperature and its set-point at the end of the control step (neglecting internal heat gains and heat exchanges between the zone and neighbouring zones or the ambient).

$$\min_{(\hat{T}_j, P_j, \epsilon_{inf,j}, \epsilon_{sup,j}) \in \{1, \dots, 4\}} \sum_{j=1}^4 (\alpha \epsilon_{inf,j} + \epsilon_{sup,j}) \quad (11)$$

$$s. t. \quad \sum_{j=1}^4 P_j = P_{Dispatch} \quad (12)$$

$$\forall j \in \{1, \dots, 4\}: 0 \leq P_j \leq P_{rated,j} \quad (13)$$

$$\hat{T}_j = T_j + P_j \frac{T_c}{C_j} \quad (14)$$

$$\epsilon_{inf,j} \geq 0 \quad (15)$$

$$\hat{T}_j + \epsilon_{inf,j} \geq T_{set,j} \quad (16)$$

$$\epsilon_{sup,j} \geq 0 \quad (17)$$

$$\hat{T}_j - \epsilon_{sup,j} \leq T_{set,j} \quad (18)$$

where for a given zone j , T_j corresponds to the measured zone temperature (obtained from the modelled temperature sensors), P_j to the actual power delivered to the heater ($P_{rated,j}$ corresponds to its rated power), C_j to the lumped heat capacity (estimated from the reduced order model), $T_{set,j}$ to the desired temperature set-point. T_c is used here

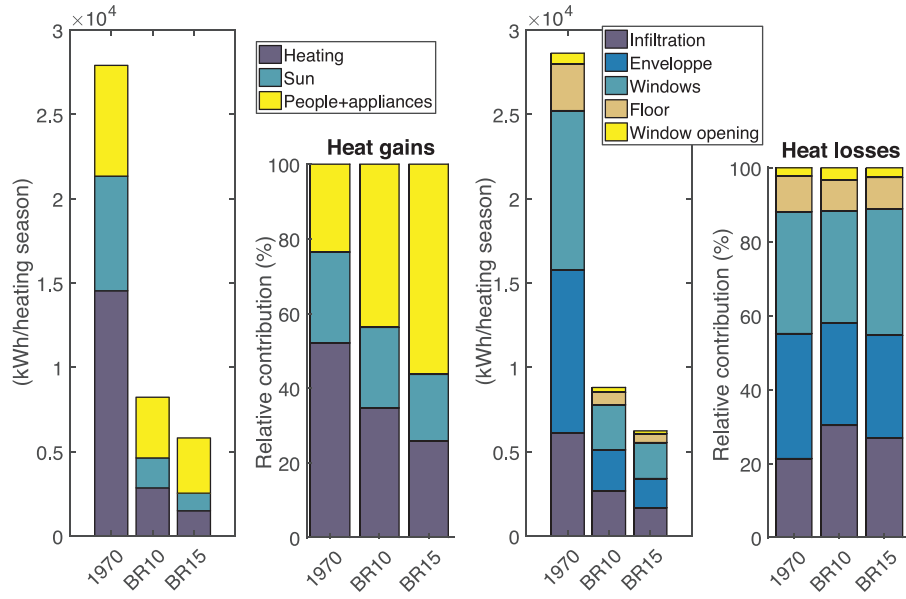


Fig. 8. Detailed summary of heat gains and losses in the simulation model for the 1970, 2010, and 2015 houses over their heating season (using the ‘Energy optimising’ predictive controller). Both absolute heat gains/losses and relative contribution of each of the losses are presented to facilitate comparison.

to denote the duration of a control step (here, $T_c = 5$ min).

The objective function (Eq. (11)) penalises the deviation below (ϵ_{inf}) and above (ϵ_{sup}) the temperature set-point of the room. A factor α is used to put a higher penalisation to under-heating (a value of 10 is used here).

The constraint in Eq. (12) imposes that the sum of all power to the heaters equals the output of the MPC (corrected by Algorithm 1). Eq. (13) ensures that the power affected to the heater in each room is within what it can deliver. Then, the constraint Eq. (14) predicts the future air temperature at the end of the time step. Here, the thermal dynamics models neglect internal heat gains and heat transfer through envelope and doors (this is reasonable over a 5 min time-step). Lastly, constraints in Eqs. ((15)–(18)) define the deviations of the future air temperature of the room below (ϵ_{inf}) and above (ϵ_{sup}) its set-point.

2.5. Quantification of performance

Here, the key performance indicators (KPIs) of the study are presented.

2.5.1. Energy consumption and CO₂ emissions

The performance of the controller was evaluated on an energy level using 2 indicators: total energy use, and CO₂ emissions. Each of these will be computed both on a monthly basis, and over the whole heating season – using Eqs. (19) and (20) below.

$$\text{Energy use } (\mathcal{T}) = T_s \sum_{k \in \mathcal{T}} U[k] \quad [\text{kWh}] \quad (19)$$

$$\text{CO}_2 \text{ emissions } (\mathcal{T}) = T_s \sum_{k \in \mathcal{T}} C_{\text{CO}_2}[k] U[k] \quad [\text{kgCO}_2, \text{eq}] \quad (20)$$

where \mathcal{T} is the period considered, T_s the duration of a simulation step, and C_{CO_2} the carbon intensity of the power (in kg CO₂ eq/kWh). Later in this work, it will be shown that it is important to consider hourly values of carbon intensity (when available) rather than a fixed factor (such as yearly average).

Lastly, an average carbon intensity of the power consumed was computed, using Eq. (21).

$$\text{Average CO}_2 \text{ intensity } (\mathcal{T}) = \frac{\text{CO}_2 \text{ emissions } (\mathcal{T})}{\text{Energy use } (\mathcal{T})} [\text{kg CO}_2, \text{eq/kWh}] \quad (21)$$

2.5.2. Indoor comfort

As explained above, indoor air temperature ranges are considered for comfort (with values from the standard EN 15251 [ENDS, 2007, Annex A3]. For the 1970 house, the range is 18–25 °C, while for the 2010/2015 houses it is 20–25 °C. Here, it is deliberately chosen to focus on occupied hours for quantifying the discomfort. This is because the occupancy of the building is assumed to be known with certainty, while the building is never left empty for more than a few hours.

From these ranges and the occupancy profile (as given in Fig. 3), the *degree hours* criterion found in EN 15251 [ENDS, 2007, Annex F] is used. This integrated occupied hot (and cold) discomfort is defined as the integral of the deviation of the indoor air temperature of the room above the upper limit (below the lower limit) of the comfort range. Here, it is important to note that the MPC is using tighter comfort bounds in the optimisation (21–24.2 °C).

For these metrics, we propose a building-wide value evaluation, by using the number of hours when at least one of the rooms has an air temperature outside the comfort range:

$$\text{Hot discomfort} = \int_{\mathcal{T}} \sigma(t) \max_j [\max(0, T_j(t) - \bar{T}_j)] dt \quad [\text{Kh}] \quad (22)$$

$$\text{Cold discomfort} = \int_{\mathcal{T}} \sigma(t) \max_j [\max(0, \underline{T}_j - T_j(t))] dt \quad [\text{Kh}] \quad (23)$$

Where σ is a function taking value 1 when the building is occupied, and 0 otherwise.

3. Results

In this section, the results of the study are presented.

3.1. Energy use in the buildings

To start with, the energy fluxes in the 3 buildings modelled were compared for the whole heating season. Compared to the 1970 house, the heat needs for the heating season were observed to be 5 times lower for the 2010 house, and almost 10 times lower for the 2015 house. The relative losses through air infiltration, envelope, windows, floor, and

window opening were roughly equivalent for all the 3 houses (Fig. 8).

Moreover, during the heating seasons, heat gains from sun, appliances, and people dominated the heat gains for the houses from 2010 and 2015, while the heating for more than half of gains for the 1970 house (Fig. 8). This emphasizes the importance of explicitly accounting for the predictable component of internal heat gains in the control model.

Considering possibilities for demand side management (including load shifting), it is clear that different building ages will have different demand response capabilities (as seen in Table 1 and later Fig. 11). First, the amount of energy that can be shifted in recent buildings is lower than in older buildings with higher heating needs. Second, the period of the year where this energy flexibility of heating is available is reduced for more recent buildings. For example, the single-family house built according to the 2015 regulations would only be able to provide demand response from heating between October and March with the weather pattern used here.

3.2. Usefulness of the power dispatcher

The power dispatcher allowed keeping a minimum temperature in each of the rooms, which significantly improved the comfort when using MPC in the 2010 and 2015 houses. With its higher heating needs and lower comfort requirements, the 1970 house was less dependent on this feature (this would be needed if the comfort requirement was increased to match the other 2 houses). This is illustrated in Fig. 9, for the case of energy optimisation (MPC-EN) with and without this feature.

As seen in Fig. 11, the total heat used for boosting is a small fraction of the total heating needs. Therefore, it is more of a ‘safety net’ for the MPC which is especially useful for energy, CO₂ and price optimisation (MPC-EN, MPC-CO₂, MPC-SPOT). It is also worth noting that comfort optimisation (MPC-COMF) is also making use of it, although less than the other MPCs.

A trade-off on the performance of the heating has been observed in the design phase when proceeding to the adjustment of minimum average temperature bound in the MPC (X_{min}). On the one hand, setting the lower bound of MPC too close to the minimum temperature for boosting triggering in the dispatcher (T_{min}) leads to extra heat being often requested, resulting in suboptimal deviations from the optimised schedule. On the other hand, setting the minimum bound in the MPC too high leads to keeping a higher average temperature (therefore

consuming more energy), but reduces the need for this potentially suboptimal boosting.

It was observed that the computation of the dispatch algorithm was very fast (much below 1 s on the laptop used for the study equipped with an Intel i7 processor), which is compatible with the real-time computing requirement.

In the rest of the experiments, the boosting was always active.

3.3. Impact of the model and prediction horizon on the controller performance

The dependency of the performance of the MPCs to the different control model structures presented in Fig. 7 was studied for the control strategies MPC-EN and MPC-CO₂ (as it was operating energy shifting) with a 24 h horizon length (N in Eq. (4)) for optimisation.

For the 1970 house, the model GB5 provided the best performance for the 1970 house, reducing energy use (−1.6% for MPC-EN) and CO₂ emissions (−1.9% for MPC-EN), respectively, compared to using GB1 – while having negligible (< 1%) adverse impact on discomfort. On the other hand, performance degradation was observed for models GB2, GB3 (higher energy use and CO₂ emissions), and GB4 (discomfort was more than doubled), compared to GB1.

For the 2010 and 2015 houses, the model GB4 was found to be the one providing the best performance. Compared to GB1, for the MPC-EN controller, energy use was reduced by 4% and 5% for the 2010 and 2015 houses, respectively – while discomfort was reduced by 8% and 8.6% respectively. Similarly, for the MPC-CO₂ controller, CO₂ emissions were reduced by 6% while discomfort was reduced by 30% for the 2010 house, and 22.5% for the 2015 house. Other models (GB2, GB3, and GB4) also provided performance improvements compared to GB1, although more limited.

A similar study was made on the horizon length with models GB5, GB4, and GB4 for the 1970, 2010, and 2015 houses, respectively. Horizon lengths of 0.5 (one step ahead optimisation in MPC), 1, 6, 12, 24, and 48 h were considered.

For the 1970 house, increase of horizon improved performance for MPC-EN (0.8–1.1% lower energy use for 24 and 48 h ahead), but degraded performance for MPC-CO₂ (0.45% higher CO₂ emissions and 37–41% increase in discomfort for 24 and 48 h horizon lengths).

For the 2010 and 2015 houses, the horizon length had little influence on the performance of MPC-EN, therefore questioning the

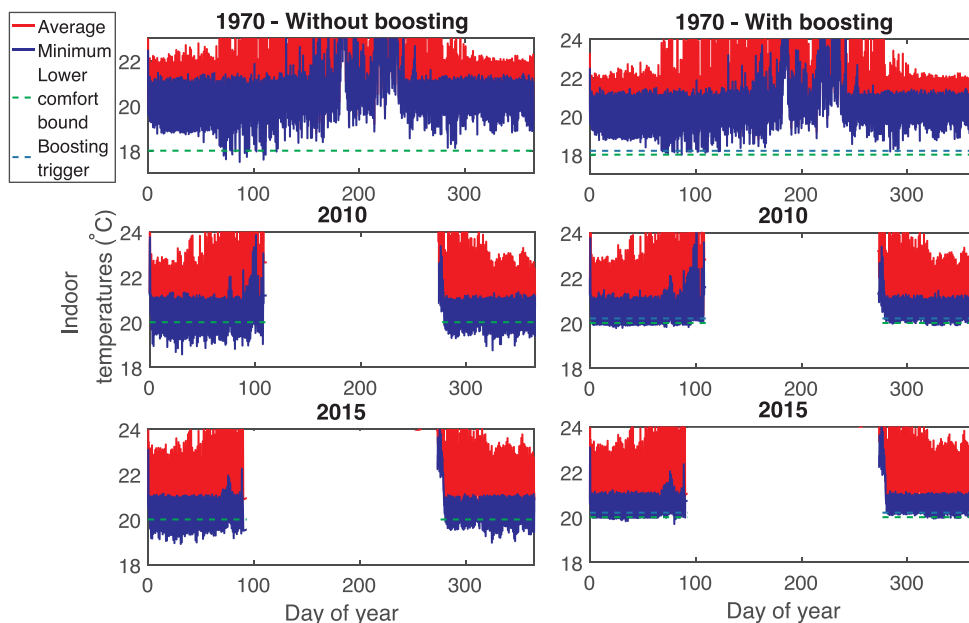


Fig. 9. Comparison of minimum and average room temperatures without (left) and with (right) boosting in the 3 houses (using MPC-EN).

relevance of MPC compared to PI control for energy optimisation. However, given the prior dependency of performance to the model, it seems that a good model is important for the state estimation which may condition the performance. For these recent buildings the MPC-CO₂ controller had best performance with a 24 h ahead horizon length (1–1.5% reduction in CO₂ emissions, with 6–10% increase in discomfort compared to a 30 min horizon length). Performance increased with horizon length up to 24 h ahead, while above 24 h it decreased again (both in terms of higher discomfort and CO₂ emissions).

Following these observations, a value of 24 h was chosen for the horizon length in the MPCs, and the models GB5, GB4, and GB4 were selected for the 1970, 2010, and 2015 houses, respectively. Here again, the solving of each step of the MPC problem with this 24 h horizon took less than a second on the laptop. Real-time computing is therefore not an issue for MPC in this form either.

3.4. Comparison of controllers

The behaviour of the thermal environment of the buildings over their heating season was then analysed for the 6 controllers (TH-REF, TH-HOT, MPC-EN, MPC-CO₂, MPC-SPOT, and MPC-COMF).

First, the thermal comfort was compared, based upon the results presented in Fig. 10. Overall, most overheating particularly occurred in the warm months (March to October for the 2010 and 2015 houses, and summer for the 1970 house for which the limits of the model are reached). It was observed that a higher thermostatic operative range (TH-HOT) range led to more hot discomfort compared to normal thermostatic operation (TH-REF). Energy optimisation (MPC-EN) reduced hot discomfort, while flexible heating using price (MPC-SPOT) or CO₂ optimisation (MPC-CO₂) led to equivalent or worse hot discomfort (especially for the 1970 house). Comfort optimisation did not reduce discomfort more than energy optimisation (which suggests that energy optimisation with a suitable lower temperature bound X_{min} is sufficient). In every case, cold discomfort was negligible, showing again the effectiveness of the boosting.

Then, the impact of the controller on the overall energy use was assessed, based upon the results of Fig. 11. For all 3 houses, relative energy savings from implementation of MPC were more marked in the spring and autumn, and lower in the winter. On a yearly basis, energy optimisation was found to reduce energy consumption by 7.7–11.3%,

compared to the thermostatic baseline. Price and CO₂ optimisation resulted in a 2.6–8.7% reduction in energy use compared to the baseline, and were always leading to higher energy consumption than the energy-optimising controller (MPC-EN), with CO₂ optimisation having an overall lower consumption than price optimisation. Comfort optimisation had a similar energy consumption to the reference thermostatic controller.

It is however important to notice that even for energy-optimal controllers, the relative savings were always less than would be observed by simply reducing the lower bound of the thermostat by 1 °C (i.e. TH-HOT to TH-REF), as this higher bound led to 12.5–25.5% higher energy use (more pronounced in the 2010 and 2015 houses).

Then focus was made on the CO₂ footprint, based upon the results displayed in Fig. 12. For the 1970 house, CO₂ optimisation was found to emit slightly (1%) more CO₂ than energy optimal strategy, which may be due to the quality of the model and highlights the practical difference between aiming for optimality and achieving it. For the houses from 2010 and 2015, CO₂ optimisation however led to the lowest CO₂ emissions (reduction compared to the baseline thermostat was 9.4% for the 2010 house, and 11.3% for the 2015 house). This reduction was however only slightly higher than for the case of energy optimisation (reduction of 8.2% and 10.3% for the 2010 and 2015 houses, respectively). In all cases, price optimisation was not found to reduce CO₂ emissions better than energy or CO₂ optimisation, and comfort optimisation did not show a significant change in footprint, compared to the baseline controller.

Here again, it is worth noting that improvements from MPC are lower than gains achieved by lowering the lower bound of the thermostatic control by 1 °C.

Detailed figures of the performance indicators for each control on each house are found in Table 3 in Appendix.

3.5. Detailed assessment of the carbon footprint

A deeper study was made on the CO₂ footprint, beyond the emission reductions from Fig. 12, to assess the potential of control to alter the correlation between load and carbon intensity in this Danish power system context.

Cross-correlations between load and carbon intensity are presented in Fig. 13, which displays both the monthly and the annual cross-

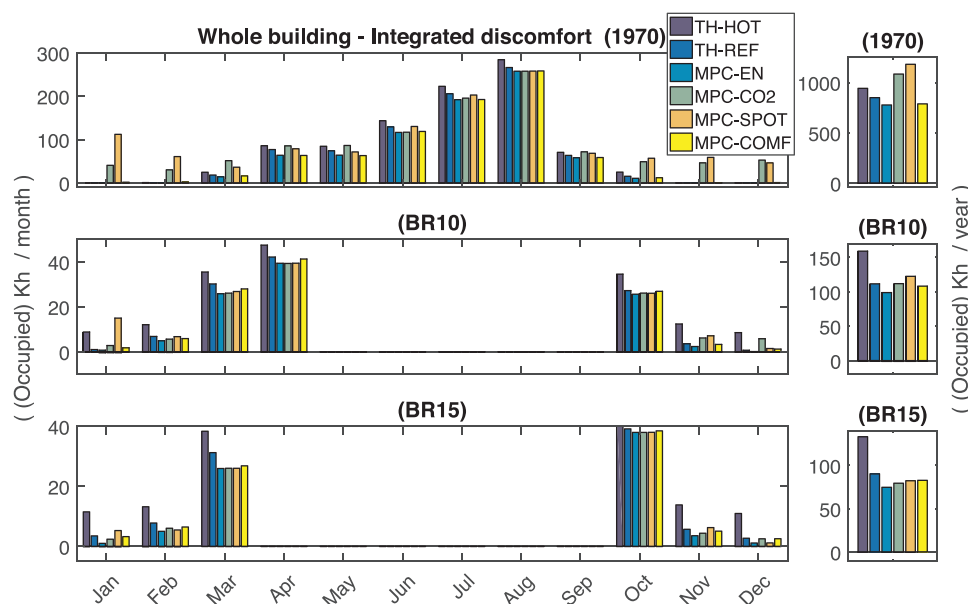


Fig. 10. Comparison of the building-wide discomfort with the different controllers the year (heating was limited to the heating season in all 3 cases, the positive component of the bars denotes hot discomfort, while the negative component denotes cold discomfort).

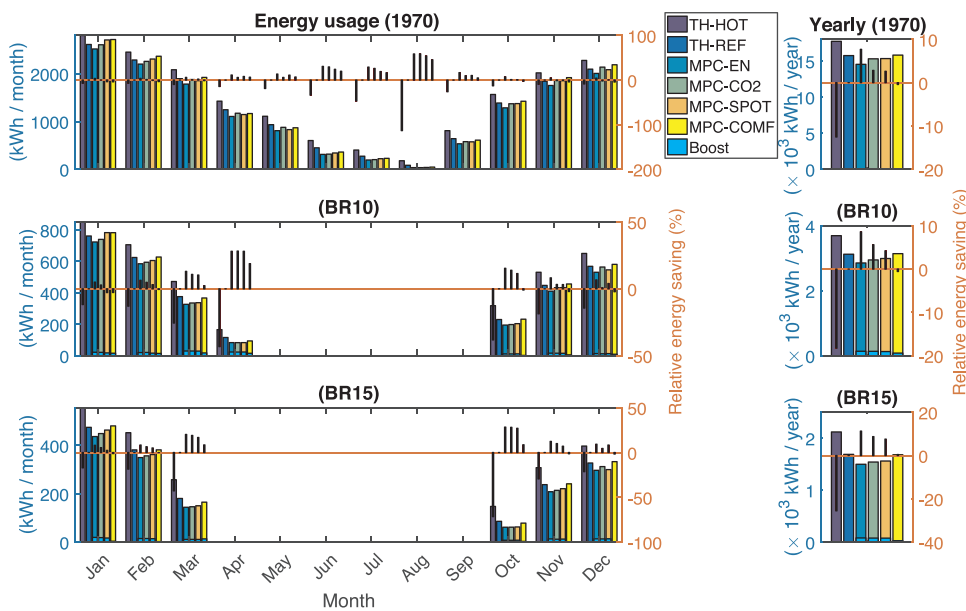


Fig. 11. Comparison of the energy consumption of each control strategy over the year (heating was limited to the heating season in all 3 cases). For each MPC controller, the amount of boosting required is shown in light blue. In order to facilitate comparison of energy consumptions, the relative savings compared to the baseline controller (TH-REF) are plotted in red. (For interpretation of the references to color in this figure legend, the reader is referred to the web version of this article.)

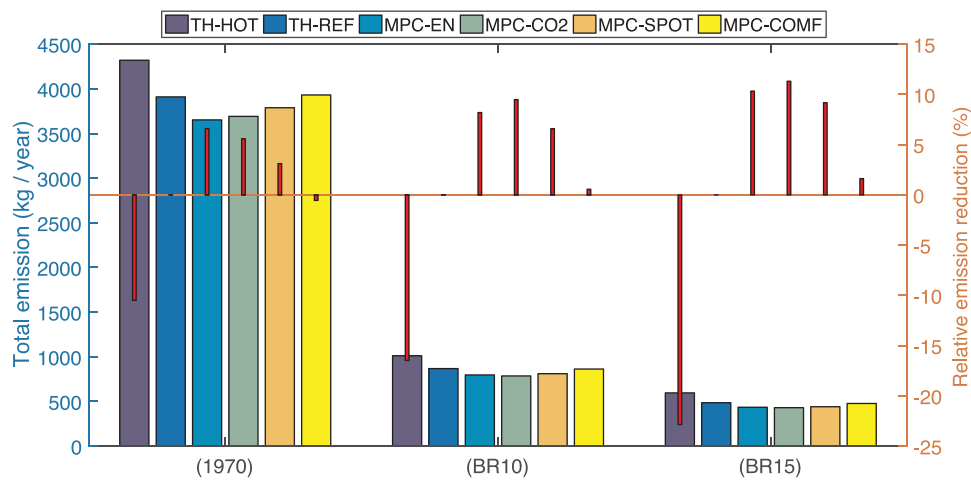


Fig. 12. Comparison of the power-related CO₂ emissions of each control strategy over the year (heating was limited to the heating season in all 3 cases).

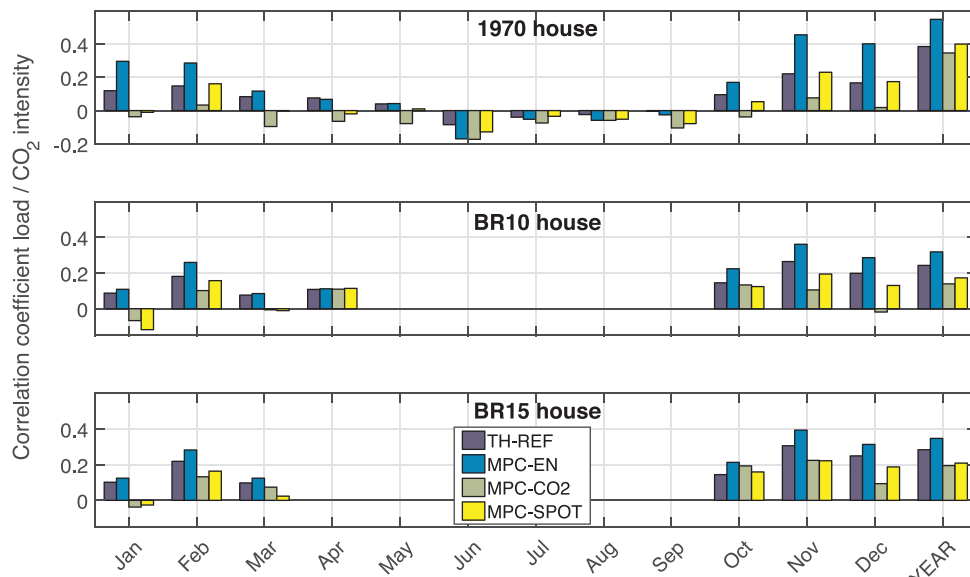


Fig. 13. Evolution of the correlation coefficients between heating load and carbon intensity over the year for the 3 houses and a selection of controllers.

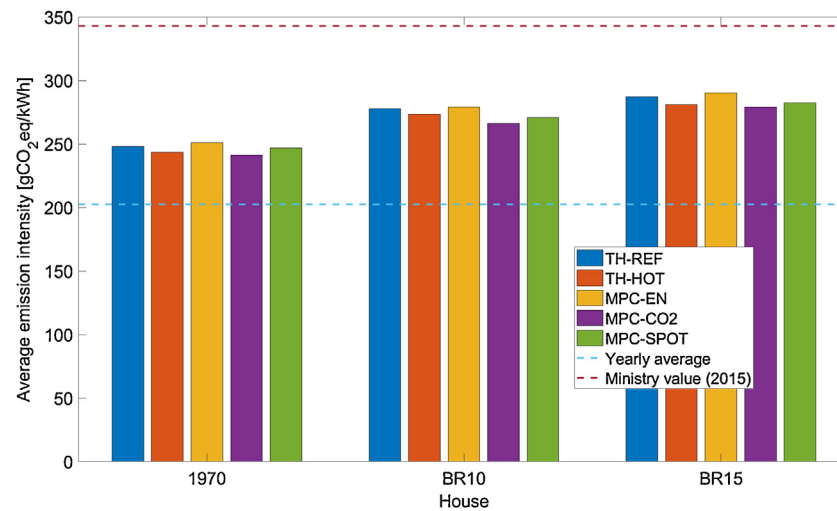


Fig. 14. Average carbon intensity for different control strategies for the 3 houses (constant factors from TSO and Energy Agency (Energistyrelsen, 2015) are provided for comparison).

correlations. In most cases, a positive correlation between load and carbon intensity was observed, and overall stronger for energy optimisation than thermostatic operation. CO₂ optimisation was observed to provide a significant decrease in this cross-correlation (and even sometimes an inversion of the correlation), especially for the 2010 and 2015 houses. For these recent houses, a similar effect was observed for price optimisation.

These cross-correlations therefore suggest that using a fixed carbon intensity factor in footprint assessment (e.g. for life-cycle assessment) leads to mis-estimations of the impact. As seen in Fig. 14, the average carbon intensity decreased with house age (as the CO₂ intensity was higher in the colder months), and was also affected by the control. It was observed that energy optimisation would typically increase the average carbon intensity compared to thermostatic control, while SPOT price optimisation would decrease it. As expected, the highest decrease of carbon intensity was achieved by CO₂ optimisation, which led to relative reductions of carbon intensity of 2.4–4.9% for the 1970 house, 1.7–4.7% for the 2010 house, and 1.1–4.0% for the 2015 house, compared to other MPC controllers and the reference thermostatic control. This explains why CO₂ optimisation consumed more energy but resulted in a lower carbon footprint for recent houses.

When assessing the total footprint, using the yearly average of the dataset resulted in 13–31% under-estimation. It was also noted that the more recent the house, the higher the under-estimation. Using the yearly average carbon intensity from the Danish Energy Agency resulted in a 18–46% over-estimation of the total footprint, with over-estimation increasing with the age of the house. This overestimation would be even higher if using a figure of 401 gCO₂eq/kWh which is proposed in another of the Agency's communications (Danish Energy Agency, 2017) (quantitative details are found in Table 2 in Appendix).

4. Discussion

4.1. On the carbon intensity metric

The carbon intensity used in this study has a number of shortcomings. First, the quantification does not account for life-cycle emissions and limits its scope to the operational emissions instead. Second, it uses a gross approximation for the emissions of the power exchanged with neighbouring countries, as imports are currently counted with the yearly averaged carbon intensity of the given country (knowing that in 2016, 21% of the power was imported from neighbouring countries, this is not negligible) (Energinet, 2017). In future works, accounting of interconnections could be improved further by using recent

developments of the 'ElectricityMap' (Tomorrow and Electricity Map), or similar solutions. A more realistic distribution loss model could be valuable, potentially integrating the effect of congestion on the local grid.

The research also identified large (> 50%) deviations between the figures of the TSO and the national Energy Agency for the the annual carbon intensity, which clearly denotes a lack of homogeneity in the quantification methods.

Moreover, looking at the impact at the societal level, marginal carbon intensity (see works of Graabak et al. (2014) and Hawkes (2010) for more details) would provide a more realistic estimate of the impact of the change in control, compared to the average carbon intensity. In such a case, the CO₂ emissions avoided through control would probably be higher, although the lack of historical data does not allow drawing a conclusion here.

Life-cycle assessments rely upon this metric to evaluate the footprint of operation of buildings. However, these typically seem to adopt a static yearly carbon intensity factor. Here (in the case of 2015), the positive correlation observed between heating load and hourly carbon intensity suggests that a simple average of carbon intensity over the year is ill-suited. In fact, where possible, it is more relevant (and precise) to use hourly carbon intensity profiles for footprint assessment. Hourly values seem particularly important when using controllers deploying energy flexibility (such as MPC), to avoid underestimating their value.

4.2. On benefits from MPC

Implementation of model predictive control was found to provide benefits compared to thermostatic control for a single-family house with low inertia heating. Strategies optimising the heating to minimise discomfort and SPOT price were not found to be bring valuable improvement (with regards to comfort, energy use, and CO₂ emissions) compared to energy and CO₂ optimisation. In fact, SPOT price optimisation provided some reduction in the average carbon intensity of power, but resulted in additional energy use leading to an overall higher footprint. However, in the eventuality of adoption of dynamic taxation to penalise CO₂ emissions further (see reference Knudsen, Hedegaard, et al., 2016 for more details), a different conclusion may be reached for price optimisation. Nevertheless, it is important to keep in mind that SPOT price optimisation provides important benefits in terms of energy costs and peak shaving (see e.g. reference Knudsen and Petersen (2016)), which were both out of the scope of this study.

Nevertheless, the reduction of energy use and footprint resulting

from implementation of MPC was lower than the reduction observed when reducing the lower bound of the thermostatic control by 1 °C. It is thus recommended to first focus on the indoor temperature set-points provided to the controller, before replacing the controller by a ‘smarter’ one.

On the one hand, dependency of the energy-optimising MPC to its horizon length highlights the limited relevance of MPC compared to Proportional Integral Derivative (PID) control for fast heaters. On the other hand, CO₂ optimisation was a very relevant use case for more recent houses, where it reduced emissions more than energy optimisation (despite higher energy needs). This was due to the reduction of the correlation between the heating load and carbon intensity of the power resulting from the load shifting (which a PID controller is not capable of supporting).

Here, it is important to bear in mind that this study focused on a low inertia heating system. It is very likely that control of heating systems with higher inertia (such as water-based floor heating with a heat-pump) would be impacted differently by implementation of MPC. As preliminary results showed, benefits from CO₂-optimising MPC might then become much more significant (e.g. reference [Vogler-Finck et al. \(2017\)](#), where CO₂ optimisation led to 10% lower emissions, compared to energy optimisation in idealised winter conditions). However, it may also be important to assess the risk of increased demand at peak load times resulting from this control (this was observed in one case by [Knudsen and Petersen \(2016\)](#)).

Lastly, use of real weather forecast and a more chaotic occupant behaviour may also lead to lower benefits. However, lower internal heat gains (compared to the rather high ones used here) could lead to more room for flexibility in energy usage, therefore accentuating differences between control strategies.

5. Conclusion

This work compared the performance of thermostatic and model predictive controllers for heating in simulations for 3 single-family houses of different construction years with several rooms. These predictive controllers were operated using a single thermal zone optimisation combined with an innovative power dispatcher ensuring minimal comfort in each room.

Predictive control provided improved performance, but only the formulations consisting in minimising energy use (for all 3 houses) and CO₂ emissions (for recent houses) and were found to be relevant when focusing solely on carbon footprint reduction and energy efficiency. These benefits vary throughout the year, with higher relative energy

savings in warmer parts of the heating season. However, these gains from implementation of such advanced controllers were comparatively smaller than those from lowering of temperature bounds of the thermostatic control to appropriate values (this should remain the priority in practice).

On such a fast heating system, MPC was not observed to bring significant improvement compared to a well-tuned PID controller for minimisation of energy use. However, for applications requiring energy shifting (such as CO₂ optimisation) in recent houses, MPC remained a means to improve performance compared to PID control.

A positive correlation was observed between carbon intensity and heating load for all controllers. This correlation was however significantly reduced by CO₂ optimisation (use of imperfect predictions of carbon intensity in this MPC may well lead to a different conclusion). Moreover, it was proposed to use a new simple metric for performance assessment of controllers making use of energy flexibility: the average carbon intensity of the power consumed over a period.

Further work should focus on extending the research to heating systems with higher inertia (e.g. water based heating, and floor heating), influence of more unpredictable occupancy and internal heat gains, adaptive update of the control model over time, use of imperfect forecast of disturbances and prices in MPC, as well as assessment of the value of using setbacks on set-points when the building is unoccupied. Furthermore, use of a more precise carbon intensity metric (including marginal emission factors) would be valuable, as such information will become more easily available and precise over time.

Acknowledgements

The authors would like to acknowledge valuable input from Kasper Vinther (formerly employed at *Aalborg University*), Søren Østergaard Jensen from the *Danish Technological Institute*, Per Dahlgaard Pedersen from *Neogrid Technologies ApS*, John Clauß from the *Norwegian University of Science and Technology*, Christian Friberg B. Nielsen from *Energinet*, Olivier Corradi from *Tomorrow*, Steffen Petersen from *Aarhus University*, as well as the anonymous reviewers of the article.

The projects *Styr din Varmepumpe (SdVP, in press)* and IEA EBC Annex 67 *Energy flexible Buildings (Jensen et al., 2017)* are also acknowledged for provision of data and inspiring discussions, respectively.

The research leading to these results is part of the ADVANTAGE project ([ADVANTAGE](#)) (funded by the European Community's Seventh Framework Programme *FP7-PEOPLE-2013-ITN* under grant agreement no. 607774).

Appendix A

Table 2

Average carbon intensity for different control strategies for the 3 houses (TSO, first and second values for Energy Agency are for 2015, 2015, and 2014, respectively).

Controller	Carbon intensity [gCO ₂ eq/kWh]		
	1970	BR10	BR15
TH-REF	248.2	277.8	287.3
MPC-EN	251.2	279.1	290.4
MPC-CO ₂	241.2	266.4	279.2
MPC-SPOT	247.0	270.9	282.4
Yearly average of TSO dataset			202.5
Danish Energy Agency (Energistyrelsen, 2015)			343
Danish Energy Agency (Danish Energy Agency, 2017)			401

Table 3

Summary of the performance indexes of the different controllers on the 3 houses over their heating season.

House	Controller	Heating energy use		Carbon footprint		Average intensity		Comfort violations	
		1000 × [kWh]		[kg CO ₂ eq]		[g CO ₂ eq/kWh]		Hot [Kh]	Cold [Kh]
1970	TH-HOT	17.7	(+ 12.0%)	4230	(+ 8.2%)			942	0.0
	TH-REF	15.8	(–)	3910	(–)	248	(–)	850	0.0
	MPC-EN	14.5	(– 8.2%)	3652	(– 6.6%)	251	(+ 1.2%)	777	0.0
	MPC-CO ₂	15.3	(– 3.2%)	3692	(– 5.6%)	241	(– 2.8%)	1084	0.0
	MPC-SPOT	15.3	(– 3.2%)	3788	(– 3.1%)	247	(– 0.4%)	1181	0.0
	MPC-COMF	15.8	(– 0.0%)	3932	(+ 0.6%)			788	0.0
2010	TH-HOT	3.70	(+ 18.2%)	1011	(+ 16.4%)			159	0.1
	TH-REF	3.13	(–)	868	(–)	278	(–)	112	0.0
	MPC-EN	2.86	(– 8.6%)	797	(– 8.2%)	279	(+ 0.4%)	99	1.2
	MPC-CO ₂	2.95	(– 5.8%)	785	(– 9.6%)	266	(– 4.3%)	112	1.2
	MPC-SPOT	2.99	(– 4.5%)	811	(– 6.6%)	271	(– 2.5%)	123	1.3
	MPC-COMF	3.14	(+ 0.3%)	863	(– 0.6%)			108	0.1
2015	TH-HOT	2.12	(+ 25.4%)	596	(+ 22.9%)			133	0.2
	TH-REF	1.69	(–)	485	(–)	287	(–)	90	0.0
	MPC-EN	1.50	(– 11.2%)	435	(– 10.3%)	290	(+ 1.0%)	75	0.3
	MPC-CO ₂	1.54	(– 8.9%)	430	(– 11.3%)	279	(– 2.8%)	80	0.3
	MPC-SPOT	1.56	(– 7.7%)	441	(– 9.1%)	282	(– 1.7%)	82	0.3
	MPC-COMF	1.68	(– 0.6%)	477	(– 1.6%)			83	0.0

References

- ADVANTAGE project website. <http://www.fp7-advantage.eu/>.
- Afram, A., & Janabi-Sharifi, F. (2014). Theory and applications of HVAC control systems – A review of model predictive control (MPC). *Building and Environment*, 72(November), 343–355. <https://doi.org/10.1016/j.buildenv.2013.11.016>.
- Andersen, R. V., Toftum, J., Andersen, K. K., & Olesen, B. W. (2009). Survey of occupant behaviour and control of indoor environment in Danish dwellings. *Energy and Buildings*, 41(1), 11–16. <https://doi.org/10.1016/j.enbuild.2008.07.004>.
- Andersen, R., Fabi, V., Toftum, J., Corgnati, S. P., & Olesen, B. W. (2013). Window opening behaviour modelled from measurements in Danish dwellings. *Building and Environment*, 69, 101–113. <https://doi.org/10.1016/j.buildenv.2013.07.005>.
- Atam, E., & Helsen, L. (2016). Control-oriented thermal modeling of multizone buildings: Methods and issues. *IEEE Control Systems Magazine*, 36(May (3)), 87–111. <https://doi.org/10.1109/MCS.2016.2535913>.
- Bacher, P., & Madsen, H. (2011). Identifying suitable models for the heat dynamics of buildings. *Energy and Buildings*, 43(7), 1511–1522. <https://doi.org/10.1016/j.enbuild.2011.02.005>.
- Bianchini, G., Casini, M., Vicino, A., & Zarrilli, D. (2016). Demand-response in building heating systems: A model predictive control approach. *Applied Energy*, 168, 159–170. <https://doi.org/10.1016/j.apenergy.2016.01.088>.
- Clauß, J., Finck, C., Vogler-Finck, P., & Beagon, P. (2017). Control strategies for building energy systems to unlock demand side flexibility – A review. *Building simulation conference 2017* <http://researchrepository.ucd.ie/handle/10197/9016>.
- Danish Energy Agency (2017). *Key figures*. <https://ens.dk/en/our-services/statistics-data-key-figures-and-energy-maps/>.
- De Coninck, R., Magnusson, F., Åkesson, J., & Helsen, L. (2015). Toolbox for development and validation of grey-box building models for forecasting and control. *Journal of Building Performance Simulation*, (August), 1–16. <https://doi.org/10.1080/19401493.2015.1046933>.
- De Coninck, R. (2015). *Grey-box based optimal control for thermal systems in buildings unlocking energy efficiency and flexibility*. Ph.D. thesis. KU Leuven.
- Delft Andersen, P., José Jiménez, M., Madsen, H., & Rode, C. (2014). Characterization of heat dynamics of an arctic low-energy house with floor heating. *Building Simulation*, 595–614. <https://doi.org/10.1007/s12273-014-0185-4>.
- Dounis, A., & Caraiscos, C. (2009). Advanced control systems engineering for energy and comfort management in a building environment – A review. *Renewable and Sustainable Energy Reviews*, 13(6–7), 1246–1261. <https://doi.org/10.1016/j.rser.2008.09.015>.
- Drgona, J., Kvasnica, M., Klauco, M., & Fikar, M. (2013). Explicit stochastic MPC approach to building temperature control. *52nd IEEE conference on decision and control (pp. 6440–6445)*. <https://doi.org/10.1109/CDC.2013.6760908>.
- DS 469: *Varme-og køleanlæg i bygninger*, Tech. rep. Dansk Standard.
- Dyson, A. A. (2016). *Energy reduction in domestic homes using smart control systems*, Ph.D. thesis. University of Leeds.
- EN ISO 7730 (2005). *Ergonomics of the thermal environment – Analytical determination and interpretation of thermal comfort using calculation of the PMV and PPD indices and local comfort criteria*, Tech. rep. ISO.
- EN/DS 15251 – *Indoor environmental input parameters for design and assessment of energy performance of buildings addressing indoor air quality, thermal environment, lighting and acoustics*, Tech. rep. Dansk Standard.
- Retningslinjer for miljødeklarationen for el, Tech. rep., Energinet.dk, Fredericia. <https://energinet.dk/-/media/Energinet/El-RGD/Retningslinjer-for-miljodeklarationen-for-el.pdf?la=da>.
- Energistatistik (2015). *Energistatistik 2015*, Tech. rep., Copenhagen.
- European Commission, Energy Efficiency Directive. <https://ec.europa.eu/energy/en/topics/energy-efficiency>.
- European Commission, Renewable Energy Directive. <https://ec.europa.eu/energy/en/topics/energy-efficiency/energy-efficiency-directive>.
- Fabietti, L. (2014). *Control of HVAC systems via explicit and implicit MPC: An experimental case study*, M.sc. thesis. KTH.
- Ferracuti, F., Fonti, A., Ciabattoni, L., Pizzuti, S., Arteconi, A., Helsen, L., & Comodi, G. (2017). Data-driven models for short-term thermal behaviour prediction in real buildings. *Applied Energy*, 204, 1375–1387. <https://doi.org/10.1016/j.apenergy.2017.05.015>.
- Fischer, D., & Madani, H. (2017). On heat pumps in smart grids: A review. *Renewable and Sustainable Energy Reviews*, 70(November), 342–357. <https://doi.org/10.1016/j.rser.2016.11.182>.
- Fonti, A., Comodi, G., Pizzuti, S., Arteconi, A., & Helsen, L. (2017). Low order grey-box models for short-term thermal behavior prediction in buildings. *Energy Procedia*, 105(June), 2107–2112. <https://doi.org/10.1016/j.egypro.2017.03.592>.
- Gearhart, J. L., Adair, K. L., Detry, R. J., Durfee, J. D., Katherine, A., & Martin, N. (2013). *Comparison of open-source linear programming solvers (October)*. 1–62.
- Graabak, I., Bakken, B. H., & Feilberg, N. (2014). Zero emission building and conversion factors between electricity consumption and emissions of greenhouse gases in a long term perspective. *Environmental and Climate Technologies*, 13(1), 12–19. <https://doi.org/10.2478/rtruet-2014-0002>.
- Gurobi Optimization Inc (2017). *Gurobi optimizer reference manual (version 6.5.1)*. <http://www.gurobi.com>.
- Hawkes, A. (2010). Estimating marginal CO₂ emissions rates for national electricity systems. *Energy Policy*, 38(10), 5977–5987. <https://doi.org/10.1016/j.enpol.2010.05.053>.
- Energy policies of IEA countries – Denmark 2017, Tech. rep. International Energy Agency (IEA).
- IEA, IPEEC (2015). *Building energy performance metrics*, Tech. rep. IEA; IPEEC.
- IEA (2017). *Denmark – Energy system overview*, Tech. rep. International Energy Agency <https://www.iea.org/media/countries/Denmark.pdf>.
- Jensen, S. Ø., Marszał-Pomianowska, A., Lollini, R., Pasut, W., Knotzer, A., Engelmann, P., Stafford, A., & Reyniers, G. (2017). IEA EBC Annex 67 Energy Flexible Buildings. *Energy and Buildings*, 155, 25–34. <https://doi.org/10.1016/j.enbuild.2017.08.044>.
- Jensen, S. Ø. (2017). *House models for Dymola to be used in connection with the OPSYS test rig and annual simulations of the performance of heat pumps*, Tech. Rep. Danish Technological Institute.
- Jiménez, M. J., Madsen, H., & Andersen, K. K. (2008). Identification of the main thermal characteristics of building components using MATLAB. *Building and Environment*, 43, 170–180. <https://doi.org/10.1016/j.buildenv.2006.10.030>.
- Knudsen, M. D., & Petersen, S. (2016). Demand response potential of model predictive control of space heating based on price and carbon dioxide intensity signals. *Energy and Buildings*, 125, 196–204. <https://doi.org/10.1016/j.enbuild.2016.04.053>.
- Knudsen, H. N., Andersen, R. K., Hansen, A. R., & Gram-Hanssen, K. (2016). House owners' interests and actions in relation to indoor temperature, air quality and energy consumption henrik. *CLIMA 2016 – Proceedings of the 12th REHVA World Congress*.
- Knudsen, M. D., Hedegaard, R. E., Pedersen, T. H., & Petersen, S. (2016). Model predictive control of space heating and the impact of taxes on demand response: A simulation study. *CLIMA 2016 – Proceedings of the 12th REHVA World Congress*.
- Li, X., & Wen, J. (2014). Review of building energy modeling for control and operation. *Renewable and Sustainable Energy Reviews*, 37, 517–537. <https://doi.org/10.1016/j.rser.2014.05.015>.

- rser.2014.05.056.
- Ljung, L. (1999). *System identification: Theory for the user* (2nd Edition). Prentice-Hall.
- Ljung, L. (2016). *MATLAB system identification toolbox™— Getting started guide R2016b (Version 9.5)*, Tech. rep. MathWorks.
- Lund, P. D., Lindgren, J., Mikkola, J., & Salpakari, J. (2015). Review of energy system flexibility measures to enable high levels of variable renewable electricity. *Renewable and Sustainable Energy Reviews*, 45, 785–807. <https://doi.org/10.1016/j.rser.2015.01.057>.
- Maasoumy Haghighi, M. (2013). *Controlling energy-efficient buildings in the context of smart grid: A cyber physical system approach*, Ph.D. thesis. Berkeley: University of California.
- Maciejowski, J. M. (2002). *Predictive control: With constraints*. Prentice Hall.
- Madsen, H., Bacher, P., Bauwens, G., Deconinck, A.-H., Reynders, G., Roels, S., Himpe, E., & Lethé, G. (2016). *Thermal Performance Characterization using Time Series Data; IEA EBC Annex 58 Guidelines* (November 28). <http://www.kuleuven.be/bwf/projects/annex58/index.htm>.
- Masy, G., Georges, E., Verhelst, C., Lemort, V., & André, P. (2015). Smart grid energy flexible buildings through the use of heat pumps and building thermal mass as energy storage in the Belgian context. *Science and Technology for the Built Environment*, 21(6), 800–811. <https://doi.org/10.1080/23744731.2015.1035590>.
- Morel, N., Bauer, M., El-Khoury, M., & Krauss, J. (2001). NEUROBAT, a predictive and adaptive heating control system using artificial neural networks. *International Journal of Solar Energy*, 21(2–3), 161–201. <https://doi.org/10.1080/0142591010891437>.
- Nägele, F., Kasper, T., & Girod, B. (2017). Turning up the heat on obsolete thermostats: A simulation-based comparison of intelligent control approaches for residential heating systems. *Renewable and Sustainable Energy Reviews*, 75(July), 1254–1268. <https://doi.org/10.1016/j.rser.2016.11.112>.
- Nygård Fergusson, A. M. (1990). *Predictive thermal control of building systems*, Ph.D. thesis. Ecole Polytechnique Federale de Lausanne.
- Oldewurtel, F. (2011). *Stochastic model predictive control for energy efficient building climate control*, Ph.D. thesis. ETH Zürich.
- OPSYS (Under floor heating and heat pump optimization) project website. <https://www.dti.dk/projects/project-under-floor-heating-and-heat-pump-optimization/37435>.
- Pedersen, T. H., Hedegaard, R. E., & Petersen, S. (2017). Space heating demand response potential of retrofitted residential apartment blocks. *Energy and Buildings*, 141, 158–166. <https://doi.org/10.1016/j.enbuild.2017.02.035>.
- Privara, S., Cigler, J., Váňa, Z., Oldewurtel, F., Sagerschnig, C., & Žáčková, E. (2013). Building modeling as a crucial part for building predictive control. *Energy and Buildings*, 56, 8–22. <https://doi.org/10.1016/j.enbuild.2012.10.024>.
- Privara, S., Šíroký, J., Ferkl, L., & Cigler, J. (2011). Model predictive control of a building heating system: The first experience. *Energy and Buildings*, 43(2–3), 564–572. <https://doi.org/10.1016/j.enbuild.2010.10.022>.
- Reynders, G., Diriken, J., & Saelens, D. (2014). Quality of grey-box models and identified parameters as function of the accuracy of input and observation signals. *Energy and Buildings*, 82, 263–274. <https://doi.org/10.1016/j.enbuild.2014.07.025>.
- Shaikh, P. H., Nor, N. B. M., Nallagownden, P., Elamvazuthi, I., & Ibrahim, T. (2014). A review on optimized control systems for building energy and comfort management of smart sustainable buildings. *Renewable and Sustainable Energy Reviews*, 34, 409–429. <https://doi.org/10.1016/j.rser.2014.03.027>.
- Styr din Varmepumpe project website. <https://styrdinvarmepumpe.dk/>.
- Tomorrow, Electricity Map | Live CO₂ emissions of electricity consumption. <http://www.electricitymap.org>.
- Twidell, J., & Weir, T. (2006). *Renewable energy resources* (2nd Edition). Taylor & Francis.
- Vinther, K., Green, T., Jensen, S.Ø., & Bendtsen, J. (2017). Predictive control of hydronic floor heating systems using neural networks and genetic algorithms. *20th IFAC world congress*.
- Vogler-Finck, P. J. C., Pedersen, P. D., Popovski, P., & Wisniewski, R. (2017). Comparison of strategies for model predictive control for home heating in future energy systems. *IEEE PowerTech* (pp. 1–6). <https://doi.org/10.1109/PTC.2017.7979747>.